

AD-766 654

ELECTRON DENSITY MEASUREMENTS AT HIGH  
PRESSURES

William H. Rudderow

Advanced Technology Center, Incorporated

Prepared for:

Air Force Cambridge Research Laboratories

June 1973

DISTRIBUTED BY:

**NTIS**

**National Technical Information Service**  
**U. S. DEPARTMENT OF COMMERCE**  
5285 Port Royal Road, Springfield Va. 22151

AD 76654

ELECTRON DENSITY MEASUREMENTS

AT HIGH PRESSURES

by

William H. Rudderow

Advanced Technology Center, Inc.  
P. O. Box 6144  
Dallas, Texas 75222

Contract No. F19628-73-C-0140  
Project No. 4642  
Task No. 464203  
Work Unit No. 46420301

Scientific Report No. 1

June 1973

Contract Monitor: Walter Rotman  
Microwave Physics Laboratory  
Approved for public release; distribution unlimited

Prepared for

Air Force Cambridge Research Laboratories  
Air Force Systems Command  
United States Air Force  
Bedford, Massachusetts 01730

Reproduced by  
NATIONAL TECHNICAL  
INFORMATION SERVICE  
US Department of Commerce  
Springfield, VA. 22151

DDC  
RECEIVED  
SEP 25 1973  
B



**ADVANCED  
TECHNOLOGY CENTER, INC.**

A SUBSIDIARY OF  
LTV AEROSPACE CORPORATION

DALLAS, TEXAS

ACCESSION FOR		
NTIS	White Section	<input checked="" type="checkbox"/>
DTC	Full Section	<input type="checkbox"/>
UNCLASSIFIED		<input type="checkbox"/>
JUSTIFICATION .....		
BY .....		
DISTRIBUTION/AVAILABILITY CODES		
Dist. Avail. and/or SPECIAL		
A		

Qualified requestors may obtain additional copies from the Defense Documentation Center. All others should apply to the National Technical Information Service.

Unclassified

Security Classification

DOCUMENT CONTROL DATA - R & D		
<i>(Security classification of title, body of abstract and indexing annotation must be entered when the overall report is classified)</i>		
1. ORIGINATING ACTIVITY (Corporate author) Advanced Technology Center, Inc. P.O. Box 6144 Dallas, Texas 75222		2a. REPORT SECURITY CLASSIFICATION Unclassified
		2b. GROUP
3. REPORT TITLE ELECTRON DENSITY MEASUREMENTS AT HIGH PRESSURES		
4. DESCRIPTIVE NOTES (Type of report and inclusive dates) Scientific Interim		
5. AUTHOR(S) (First name, middle initial, last name) William H. Rudderow		
6. REPORT DATE June 1973	7a. TOTAL NO. OF PAGES 24	7b. NO. OF REFS 21
8a. CONTRACT OR GRANT NO. F19628-73-C-0140	8b. ORIGINATOR'S REPORT NUMBER(S) Scientific Report No. 1 ATC Report No. B-94300/3CR-19	
b. PROJECT, TASK, AND WORK UNIT NO. 4642-03-01		
c. JOD ELEMENT 62101F		
d. DOD SUBELEMENT 684642	8c. OTHER REPORT NO(S) (Any other numbers that may be assigned this report) AFCRL-TR-73-0436	
10. DISTRIBUTION STATEMENT A - Approved for public release; distribution unlimited.		
11. SUPPLEMENTARY NOTES Tech, other		Air Force Cambridge Research Laboratories (LZ) L. G. Hanscom Field Bedford, Massachusetts 01730
13. ABSTRACT Measurements of the electron density in the flow produced by high velocity shock waves in air at initial pressures of 5 torr and 10 torr have been performed in an electromagnetic shock tube. The current collected by flush-mounted probes mounted in the wall of a rectangular cross section shock tube were used to deduce the electron density. Measurements were performed where the probes were biased to collect either ion current or electron current, and a simple theory was used to describe the probe characteristics. The flow conditions surrounding the probe were computed with engineering approximations of the wall boundary layer. A comparison of the measured results and the predicted values agree within a factor of two. Additional measurements of the current collected by a stagnation point electrostatic probe were also performed. Using simple theories, the measured electron density agrees with theoretical predictions within a factor of three.		

DD FORM 1473 NOV 65

Unclassified

Security Classification

Unclassified

Security Classification

14 KEY WORDS	LINK A		LINK B		LINK C	
	ROLE	WT	ROLE	WT	ROLE	WT
Re-entry Plasma diagnostics Electrostatic probe Shock tube						

Unclassified

Security Classification

*ib*

ELECTRON DENSITY MEASUREMENTS

AT HIGH PRESSURES

by

William H. Rudderow

Advanced Technology Center, Inc.  
P. O. Box 6144  
Dallas, Texas 75222

Contract No. F19628-73-C-0140

Project No. 4642

Task No. 464203

Work Unit No. 46420301

Scientific Report No. 1

June 1973

Contract Monitor: Walter Rotman  
Microwave Physics Laboratory

Approved for public release; distribution unlimited

Prepared for

Air Force Cambridge Research Laboratories  
Air Force Systems Command  
United States Air Force  
Bedford, Massachusetts 01730

## ABSTRACT

Measurements of the electron density in the flow produced by high velocity shock waves in air at initial pressures of 5 torr and 10 torr have been performed in an electromagnetic shock tube. The current collected by flush-mounted probes mounted in the wall of a rectangular cross section shock tube were used to deduce the electron density. Measurements were performed where the probes were biased to collect either ion current or electron current, and a simple theory was used to describe the probe characteristics. The flow conditions surrounding the probe were computed with engineering approximations of the wall boundary layer. A comparison of the measured results and the predicted values agree within a factor of two. Additional measurements of the current collected by a stagnation point electrostatic probe were also performed. Using simple theories, the measured electron density agrees with theoretical predictions within a factor of three.

## TABLE OF CONTENTS

	<u>Page</u>
ABSTRACT . . . . .	ii
LIST OF FIGURES . . . . .	iv
1.0 INTRODUCTION . . . . .	1
2.0 EXPERIMENTAL FACILITY . . . . .	1
3.0 FLUSH PROBE OPERATION . . . . .	2
3.1 Flush Probe Theory . . . . .	5
3.2 Flow Field Theory . . . . .	6
3.3 Flush Probe Measurements . . . . .	7
3.3.1 Run Time Measurements . . . . .	7
3.3.2 Electron Density Measurements . . . . .	10
4.0 STAGNATION POINT PROBE OPERATION . . . . .	14
4.1 Stagnation Point Probe Theory . . . . .	18
4.2 Stagnation Point Flow Field Theory . . . . .	18
4.3 Stagnation Point Probe Measurements . . . . .	20
5.0 CONCLUSIONS . . . . .	20
REFERENCES . . . . .	24

## LIST OF FIGURES

<u>Figure</u>		<u>Page</u>
1	Shock Tube Schematic . . . . .	3
2a	Flush Electrostatic Probe . . . . .	4
2b	Flush Electrostatic Probe Response . . . . .	4
3	Run Time, P = 10 torr . . . . .	8
4	Run Time, P = 5 torr . . . . .	9
5	Sheath Location, P = 10 torr, V = -18.6 volts . . . . .	11
6	Sheath Location, P = 10 torr, V = +18.6 volts . . . . .	12
7	Electron Density Based on Ion Current, P = 10 torr . . . . .	13
8	Electron Density Based on Electron Current, P = 10 torr . . . . .	15
9	Sheath Location, P = 5 torr, V = -12 volts . . . . .	16
10	Electron Density Based on Ion Current, P = 5 torr . . . . .	17
11a	Stagnation Point Electrostatic Probe . . . . .	19
11b	Stagnation Point Electrostatic Probe Response . . . . .	19
12	Sheath Location, P = 5 torr, V = -12 volts . . . . .	21
13	Electron Density Based on Ion Current, P = 5 torr V = -12 volts . . . . .	22

## 1.0 INTRODUCTION

The use of electrostatic probes for the measurement of electron density in hypersonic flows is well established. For continuum flows the use of flush-mounted electrostatic probes offer several advantages in the determination of the electron concentration at a particular point in the ionized gas flow. Flush probes do not interfere with the local flow and can, therefore, be used to measure electron density in regions where protruding probes would cause serious flow perturbations due to secondary shocks and related effects. Flush probe data can be analyzed with only an estimate of the temperature and mobility at the sheath edge since the charged particle density and sheath thickness are weak functions of these quantities. The validity of flush probe theory has been demonstrated in full scale flight test measurements where the results have been compared with a detailed calculation of the electron density at the sheath edge<sup>1,2</sup>. Good agreement with the probe theory of Bredfelt et al<sup>3</sup> coupled with careful calculations of the flow field has been shown for a major portion of a flight test reentry trajectory.

The experimental work described here has been designed to measure the electron density at conditions of short neutral particle mean free path lengths and high values of electron density typical of the conditions encountered during low-altitude, high-velocity reentry. The gas is assumed to be in thermodynamic equilibrium, and the results are compared with straightforward engineering calculations of a real gas flow field.

In addition to the flush mounted probe measurements, measurements of the current collected by a stagnation point probe protruding into the flow are used to deduce the electron density at the sheath edge. These results are also compared to an approximate calculation of the flow conditions at the sheath edge.

## 2.0 EXPERIMENTAL FACILITY

The experiments described here were performed in the conical-electromagnetic shock tube using room air as the test gas. The gas in the driver section is heated by electromagnetic forces which compress the gas contained in the converging conical region. After bursting a thin diaphragm, the flow expands and forms a new moving shock wave system in the driven section. The details of

the shock tube and the driving technique have been described elsewhere<sup>4</sup>.

The driven section consists of a 3.81 x 1.27 cm rectangular tube with a length of 111.5 cm. The driven section was machined from aluminum and several observation ports were located along the axis of the tube. Provisions for the installation of special dielectric test sections were also provided at two locations. A sketch of the facility is shown in Figure 1.

The pressure in the driver section was maintained at 0.5 torr and the pressure in the driven section was fixed at either 10 torr or 5 torr. Room air was used as the test gas in the driver and driven sections, and all pressures were measured with a precision capacitance-type pressure gage. The shock velocity was varied by adjusting the capacitor bank voltage to the desired level. Capacitor bank voltages from 7-9 kV provided shock velocities of 2.8-4 mm/ $\mu$ sec for the prescribed initial conditions.

The shock velocity was monitored by observing the time intervals between the output of fast-rise static pressure probes located at several locations along the axis of the shock tube. The voltage output of two static pressure probes were processed and displayed on one sweep of an oscilloscope to provide the time interval between two discrete locations. Available test time was measured by observing the onset of the shock wave and the arrival of the contact surface from the output of the electrostatic probes.

### 3.0 FLUSH PROBE OPERATION

The flush mounted electrostatic probes were constructed of a copper center electrode insulated from the shock tube wall with a Teflon spacer as shown in Figure 2a. The shock tube wall was used as a reference electrode, and the entire probe was mounted in a coaxial arrangement. The center electrode was biased relative to the shock tube wall with a battery. The collected current was measured by observing the voltage drop across a load resistor placed in the circuit. The output voltage was recorded on a dual beam oscilloscope which also displayed a velocity measurement at the axial location of the probe. The

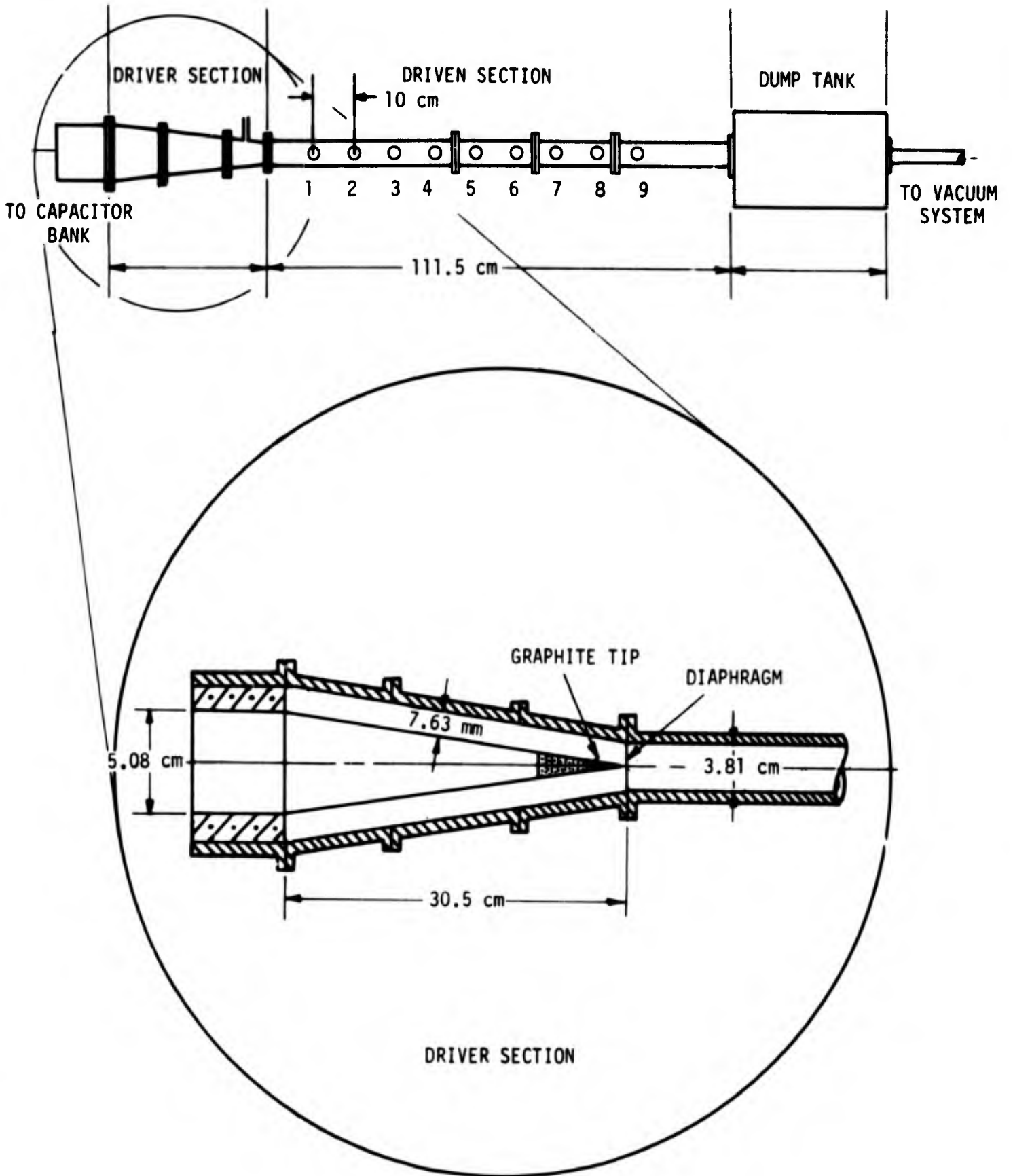


FIG. 1 SHOCK TUBE SCHEMATIC

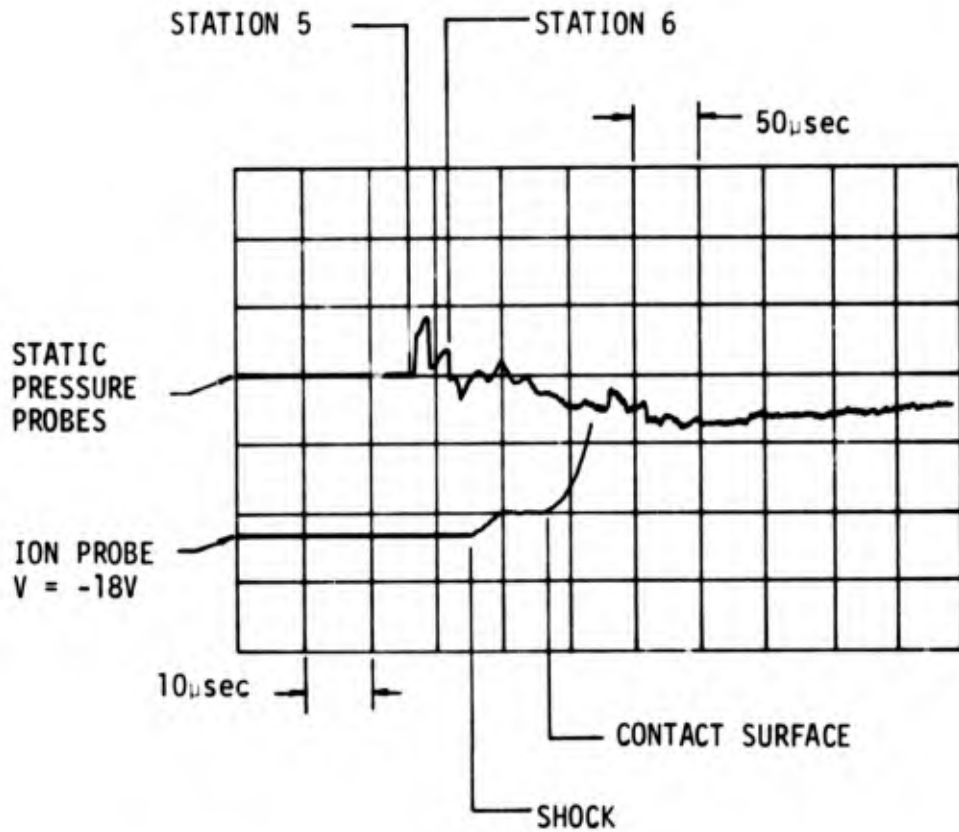
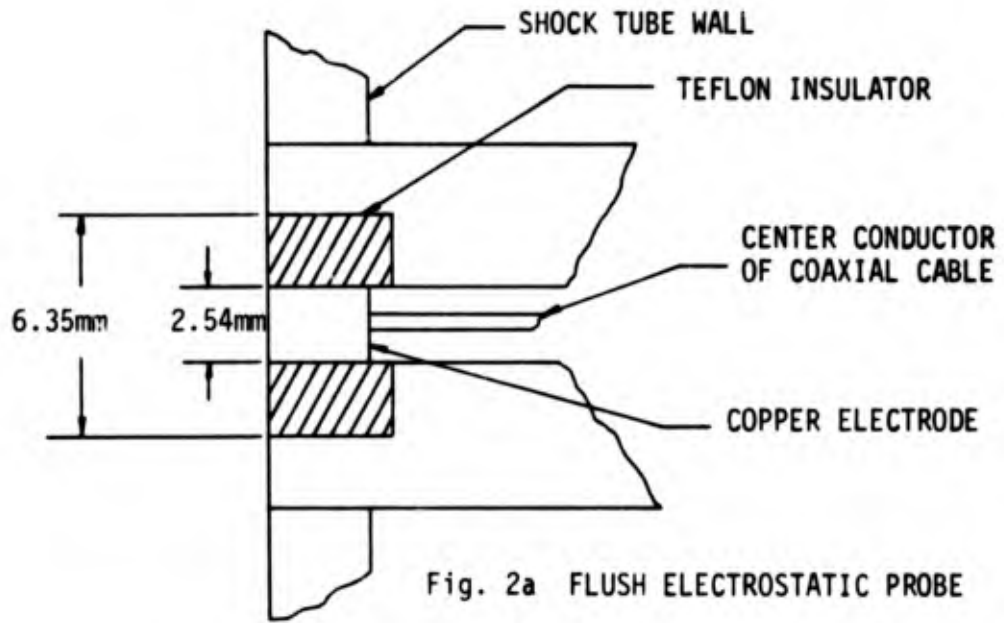


Fig. 2b FLUSH ELECTROSTATIC PROBE RESPONSE

load resistor was selected according to the expected probe current and was varied from 10 to 1000 ohms over the range of shock velocity. A typical probe response is shown in Figure 2b.

In addition to the charged particle collection the flush probes were used to define the uniform test time. The useful test time is defined as the time interval between the passage of the shock wave and the arrival of the contact surface. The test time is limited due to viscous effects along the walls of the shock tube which causes significant reductions in the theoretically available non viscous test time. For the flow conditions in the experiments described here, the losses are assumed to be due to a wall turbulent boundary layer. The theoretical test time including losses due to a turbulent boundary layer are calculated with Mirel's theory<sup>12</sup>.

### 3.1 Probe Theory

The theory of flush probe operation in an ionized gas has been studied for many years<sup>3,5-10</sup>. For completely general results the equations describing the flow field must be solved simultaneously with the electromagnetic equations describing the probe influence on the flow. Most of the analyses require a number of assumptions and a knowledge of the flow properties at the edge of the sheath. Owing to the difficulty in obtaining exact solutions, the simplified approach of Bredfelt et al<sup>3</sup> was selected as an appropriate theory to describe the probe characteristics in continuum flow.

Following Bredfelt et al, the full random current at the sheath edge is assumed to be collected by the probe,

$$j = \frac{1}{4} neV_{th} ,$$

where the charged particle thermal speed is

$$V_{th} = \left( \frac{3kT_e}{m} \right)^{1/2} .$$

The electron temperature is assumed to be equal to the gas temperature at the edge of the boundary layer. For the temperatures of interest the dominant

ion is  $\text{NO}^+$  and is considered to be the specie collected when the probe is biased negatively.

The location of the sheath edge is determined from the planar space-limited, diode relation

$$j = 9/8 \epsilon_0 \mu_s \frac{V^2}{y_s^3}$$

where  $\epsilon_0$  = permittivity of free space

$\mu_s$  = mobility of charged specie

$V$  = probe bias

$y_s$  = normal distance from probe surface to sheath edge

The ion mobility was calculated from the Langevin equation<sup>11</sup> using thermodynamic properties defined at the edge of the boundary layer. By using the measured current density and probe potential, the sheath thickness,  $y_s$ , was calculated.

### 3.2 Flow Field Theory

The flow field exposed to the flush probe is created by a moving shock wave flowing past the probe surface. Viscous effects cause a boundary layer to form next to the wall, and the probe sheath is located within the boundary layer for the prescribed experimental conditions. The boundary layer is considered to be turbulent and in thermodynamic equilibrium. The conditions at the edge of boundary layer were calculated from the real air shock tube tables of Menard and Horton<sup>13</sup>. The conditions in the boundary layer were calculated by the method outlined by Jacobs<sup>14</sup>. These calculations utilize the reference enthalpy method for defining the transport properties within the boundary layer and define the boundary layer momentum thickness with the Blasius relation. The velocity profile is assumed to follow a 1/7 power law variation, and the boundary layer thickness can then be determined from the usual relation between momentum and velocity thickness. The enthalpy profile was determined from the Crocco relationship and the fluid properties

were determined from real air thermodynamic properties<sup>15</sup>. The electron density was determined from tabulated electron concentrations<sup>16</sup> for the prescribed temperature and density within the boundary layer. The electron density was calculated for the sheath edge location determined from the experimental measurements.

### 3.3 Flush Probe Measurements

The flush mounted electrostatic probes were installed in the wall of the driven section of the shock tube. For an initial pressure of 10 torr the probe was located at an axial location of 65.4 cm from the diaphragm. For an initial pressure of 5 torr the probe was located at 84.91 cm. Piezo-electric static pressure probes were located at the same axial location as the electrostatic probe and at a position 10 cm upstream of the probe. The static pressure probe outputs were fed into a differential preamplifier and displayed on one sweep of a dual beam oscilloscope. The voltage output of the load resistor of the electrostatic probe was then fed into the second beam of the oscilloscope to provide a simultaneous measurement of shock velocity, run time, and probe current.

#### 3.3.1 Run Time Measurements

The equilibrium run time measured by the flush electrostatic probes is shown in Figure 3 as a function of velocity for an axial distance of 65.4 cm from the diaphragm. The initial pressure in the shock tube was maintained at 10 torr for these measurements. Various probe bias was used for these measurements and no effect is noticed for the range of shock velocity. The theoretical run time assuming losses due to a turbulent boundary layer<sup>12</sup> is shown for the experimental conditions. The obvious scatter of the observed data and the theoretical prediction can be attributed to the initial discharge conditions and the diaphragm opening phenomena. The over-all trend of the data does indicate the correct trend with shock velocity and validates the assumption of a turbulent boundary layer.

The run time for an initial pressure of 5 torr is shown as a function of velocity in Figure 4. The probe was located at an axial location

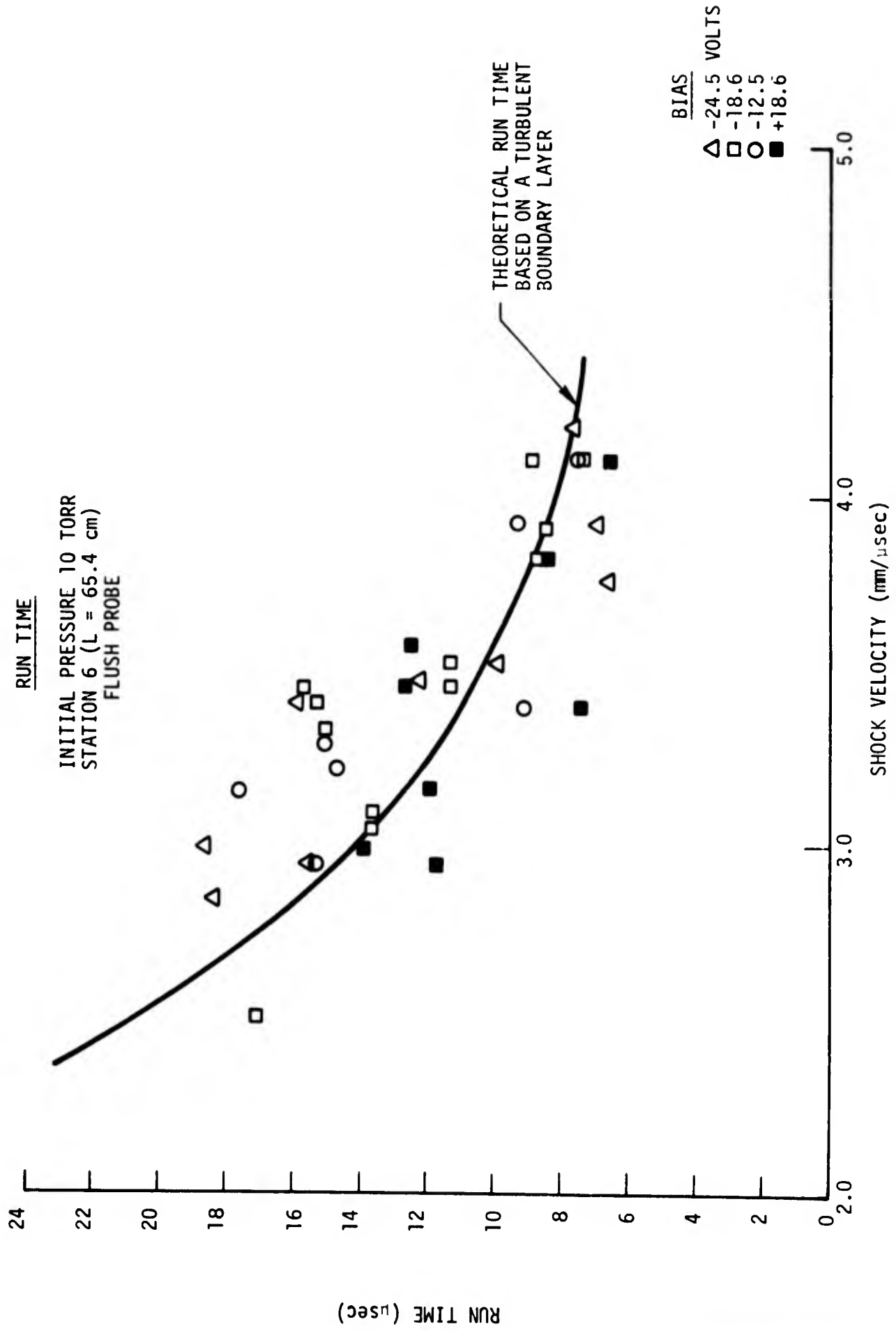


Fig. 3 RUN TIME, P = 10 TORR

RUN TIME  
FLUSH PROBE  
INITIAL PRESSURE 5.0 TORR  
PROBE BIAS -12 VOLTS  
STATION 8 (L = 84.91 cm)

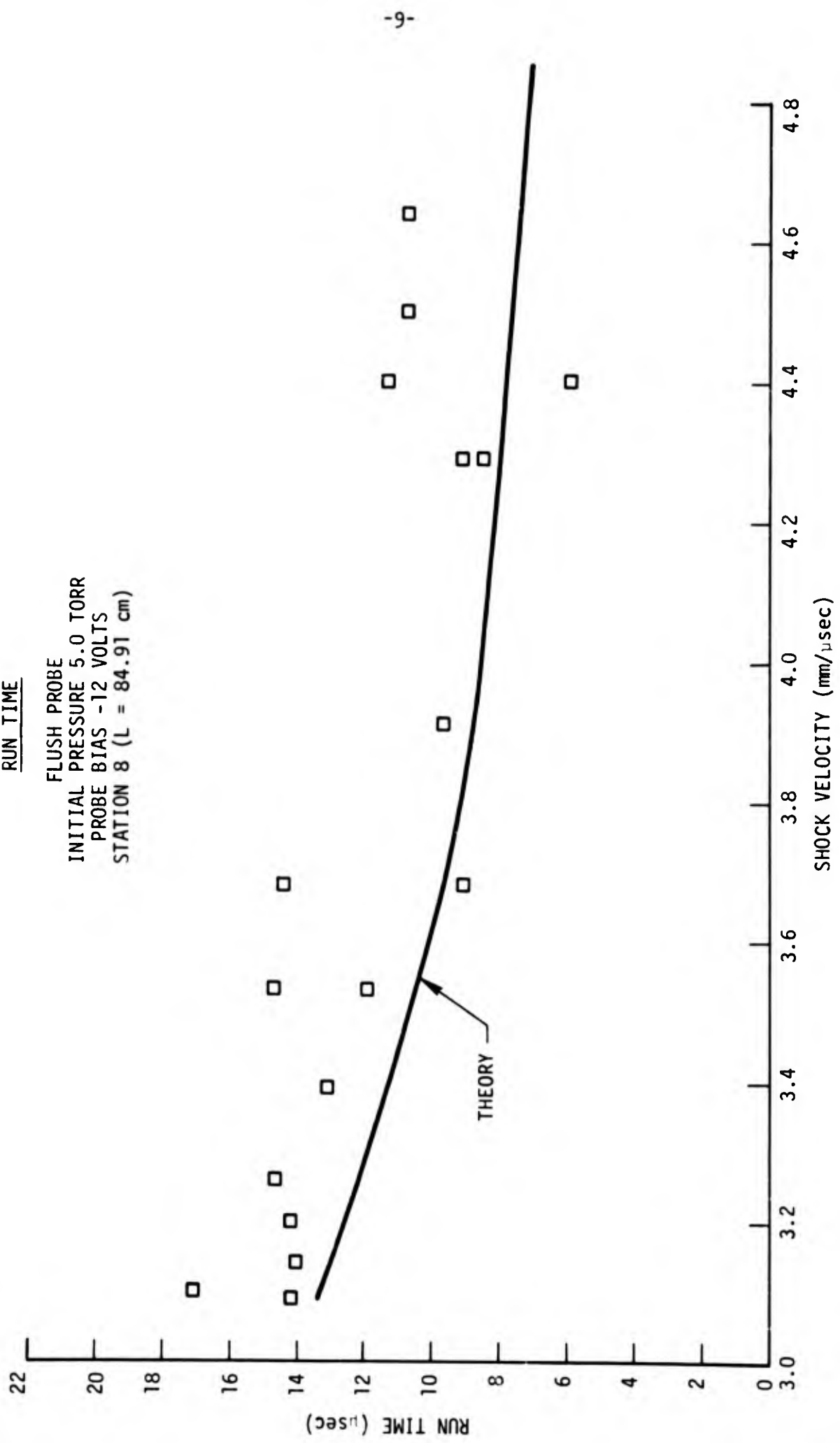


Fig. 4 RUN TIME, P = 5 TORR

of 84.91 cm and the probe bias was fixed at -12 volts. The scatter of the data with theory is similar to the 10 torr measurements, but the correct trend with shock velocity is again observed.

### 3.3.2 Electron Density Measurements

The probe current density is defined by the measured current and the geometric area of the probe. This assumption therefore neglects any fringing field effects. The sheath edge was determined from the planar diode relation using the conditions at the edge of the boundary layer to determine the charged particle mobility. The sheath edge was determined from the measured current density, probe voltage, and calculated mobility. The sheath location for a fixed probe bias of -18.6 volts and an initial shock tube pressure of 10 torr is shown as a function of shock velocity in Figure 5. A curve faired through the data points provides a mean sheath edge distance as a function of shock velocity for a fixed bias.

The sheath location for a probe biased to collect electron current is shown in Figure 6. The probe bias was maintained at +18.6 volts and the initial shock tube pressure was 10 torr. The sheath edge was calculated in a similar manner using the appropriate expression for electron mobility. The sheath thickness is shown to be slightly larger than the ion sheath thickness.

The electron density was calculated by assuming the full random flux was collected by the probe at the sheath edge. Since the sheath distance is much less than the boundary layer thickness, convective effects were neglected. The electron density deduced from the measured ion current density and the calculated mean thermal speed is shown in Figure 7 for a fixed bias of -18.6 volts and an initial shock tube pressure of 10 torr. The calculated electron density at the average location of the sheath edge is also shown as a function of velocity. The electron density profile was calculated from the turbulent boundary layer prediction and the measured average sheath location. The agreement is within a factor of two and is well within the experimental accuracy of the measurements and calculations.

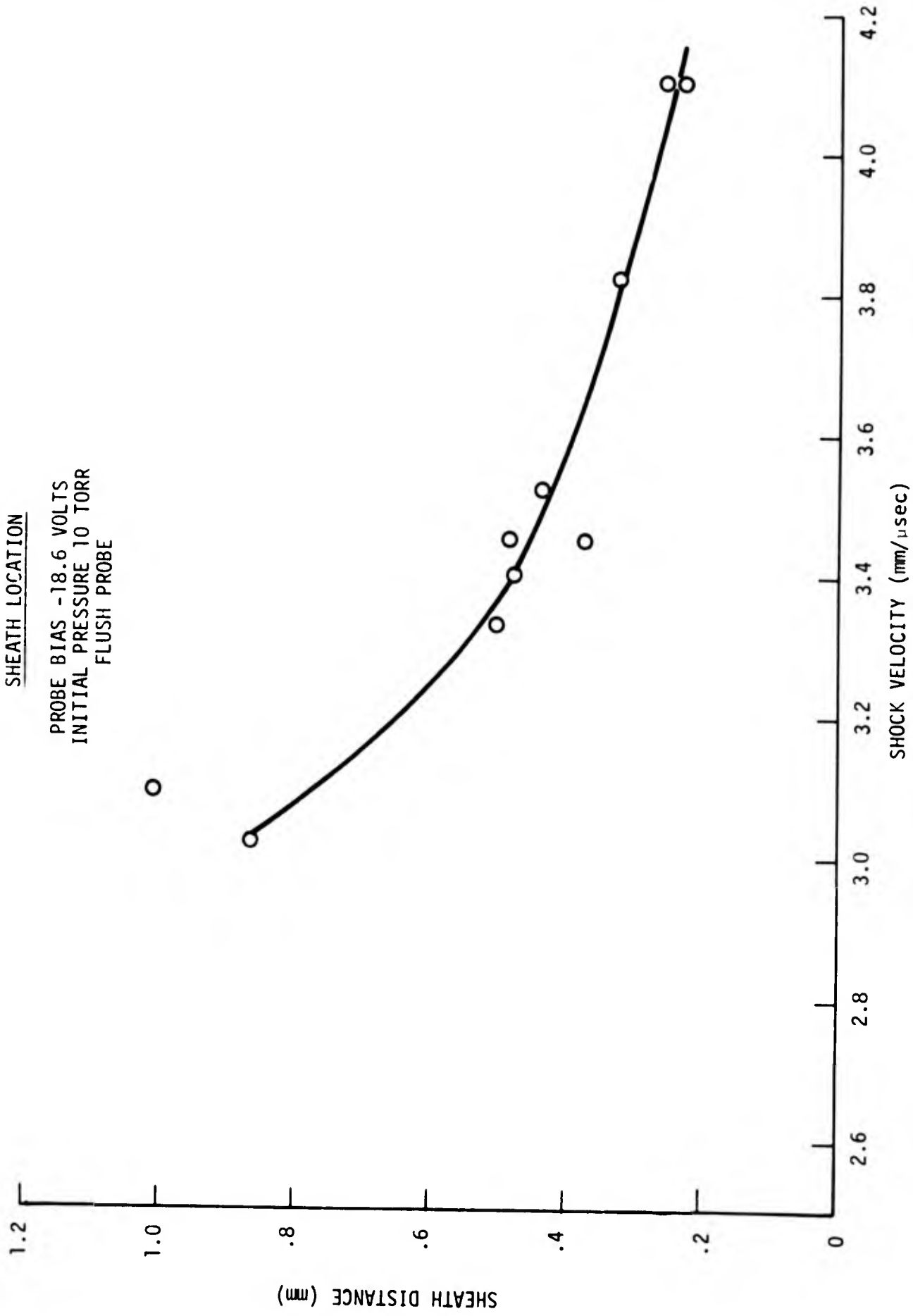
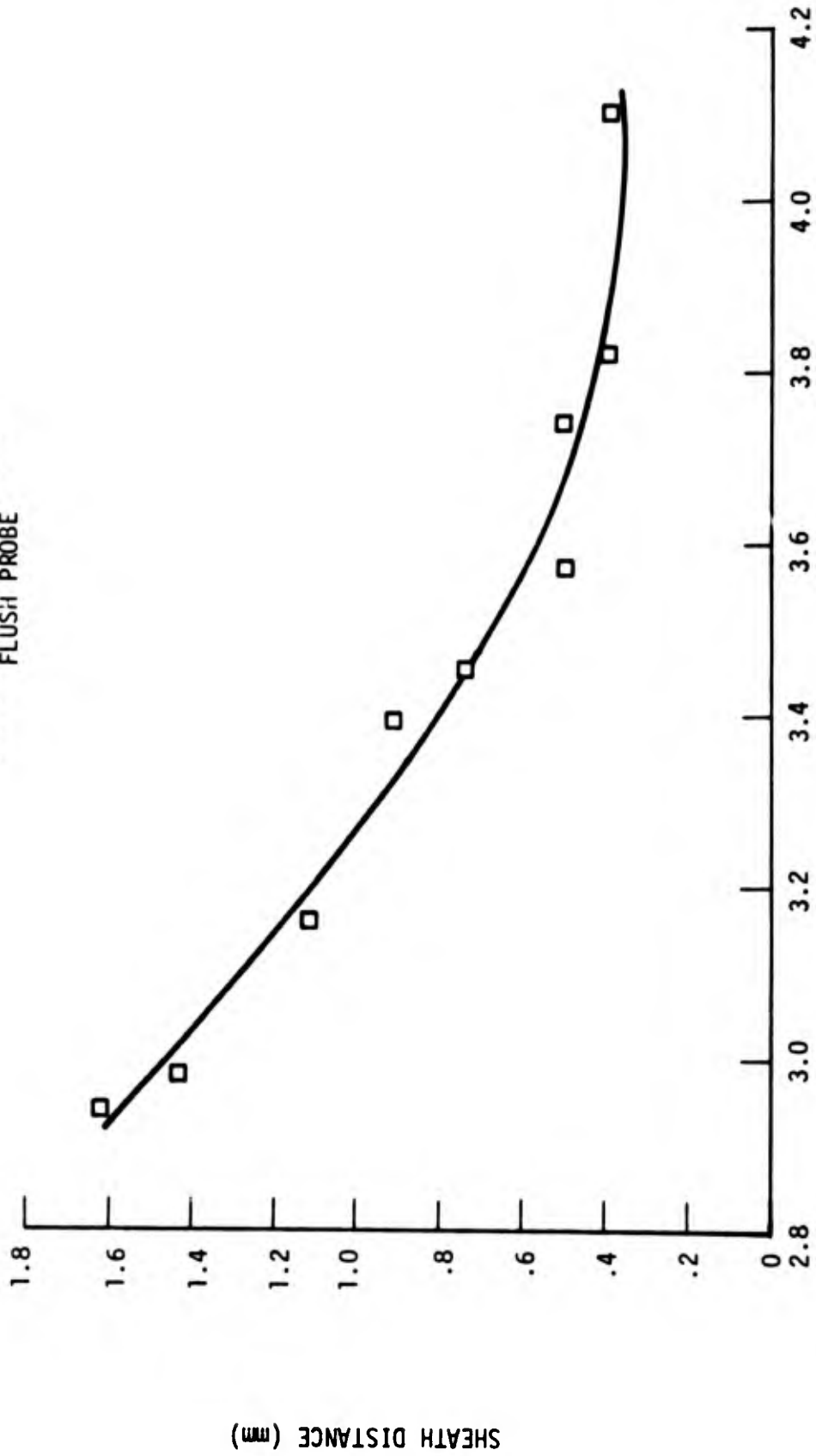


Fig. 5 SHEATH LOCATION, P = 10 TORR, V = -18.6 VOLTS

SHEATH LOCATION

PROBE BIAS +18.6 VOLTS  
INITIAL PPESSURE 10 TORR  
FLUSH PROBE



SHOCK VELOCITY (mm/μsec)

Fig. 6 SHEATH LOCATION, P = 10 TORR, V = +18.6 VOLTS

SHEATH DISTANCE (mm)

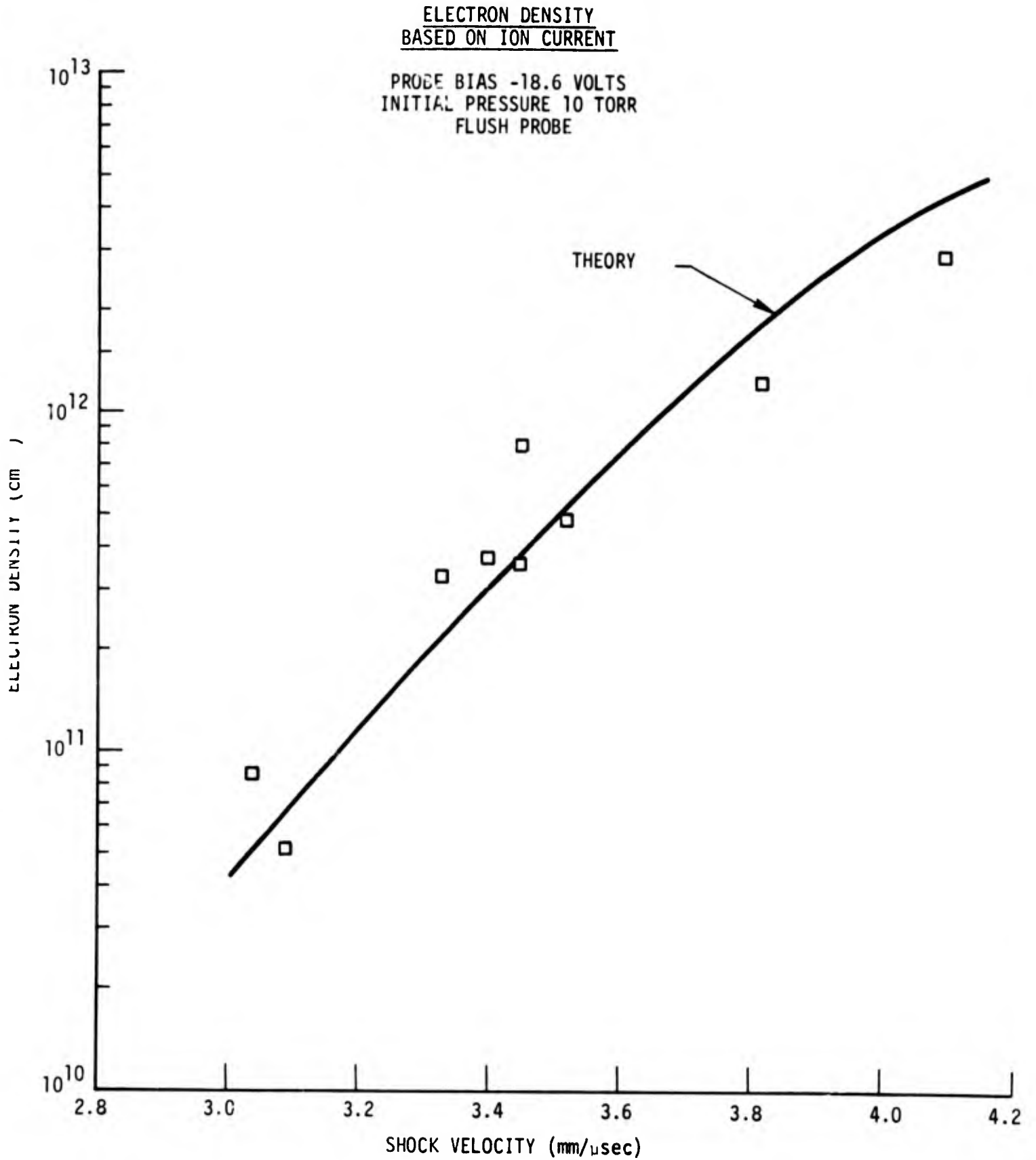


Fig. 7 ELECTRON DENSITY BASED ON ION CURRENT,  
P = 10 TORR

The electron density deduced from measurements of the probe biased to collect electron current is shown in Figure 8. The probe bias was fixed at +18.6 volts and the shock tube initial pressure was maintained at 10 torr. The agreement with theory is similar to the ion current measurements.

Measurements of the probe ion current for an initial shock tube pressure of 5 torr were also performed. The sheath edge was calculated in the same manner as the 10 torr measurements. The sheath edge is shown as a function of velocity for a fixed bias of -12 volts in Figure 9. The electron density deduced from the measured parameters is shown in Figure 10. The agreement with theoretical predictions is again within a factor of two.

#### 4.0 STAGNATION POINT PROBE OPERATION

The stagnation point electrostatic probe has been suggested as a useful means of measuring the electron density in ionized flows<sup>17,18</sup>. The operation of the stagnation point probe is similar to the flush mounted probe for the collection of probe current. The advantage of the stagnation point probe is the fact that the flow field surrounding the probe is usually known with a greater amount of confidence than flow conditions far downstream of the stagnation point. For shock tube applications, however, a shock wave will form in front of a blunt protruding probe requiring additional flow field calculations to determine boundary layer edge conditions. The non viscous flow around the probe will consist of a region between the stand-off shock and the boundary of the viscous layer. The probe sheath will extend into this region depending on the probe bias. For the experiments performed here the probe sheath thickness is less than the boundary layer thickness and the electron density will be measured within the laminar boundary layer.

The construction of the stagnation point probe is similar to the flush mounted probe with the copper center electrode biased relative to the shock tube wall. A sketch of the probe which illustrates the coaxial configuration is shown in Figure 11a. The probe was biased with a battery and the probe current was determined from the voltage drop across a load resistor inserted

ELECTRON DENSITY  
BASED ON ELECTRON CURRENT

PROBE BIAS +18.6 VOLTS  
INITIAL PRESSURE 10 TORR  
FLUSH PROBE

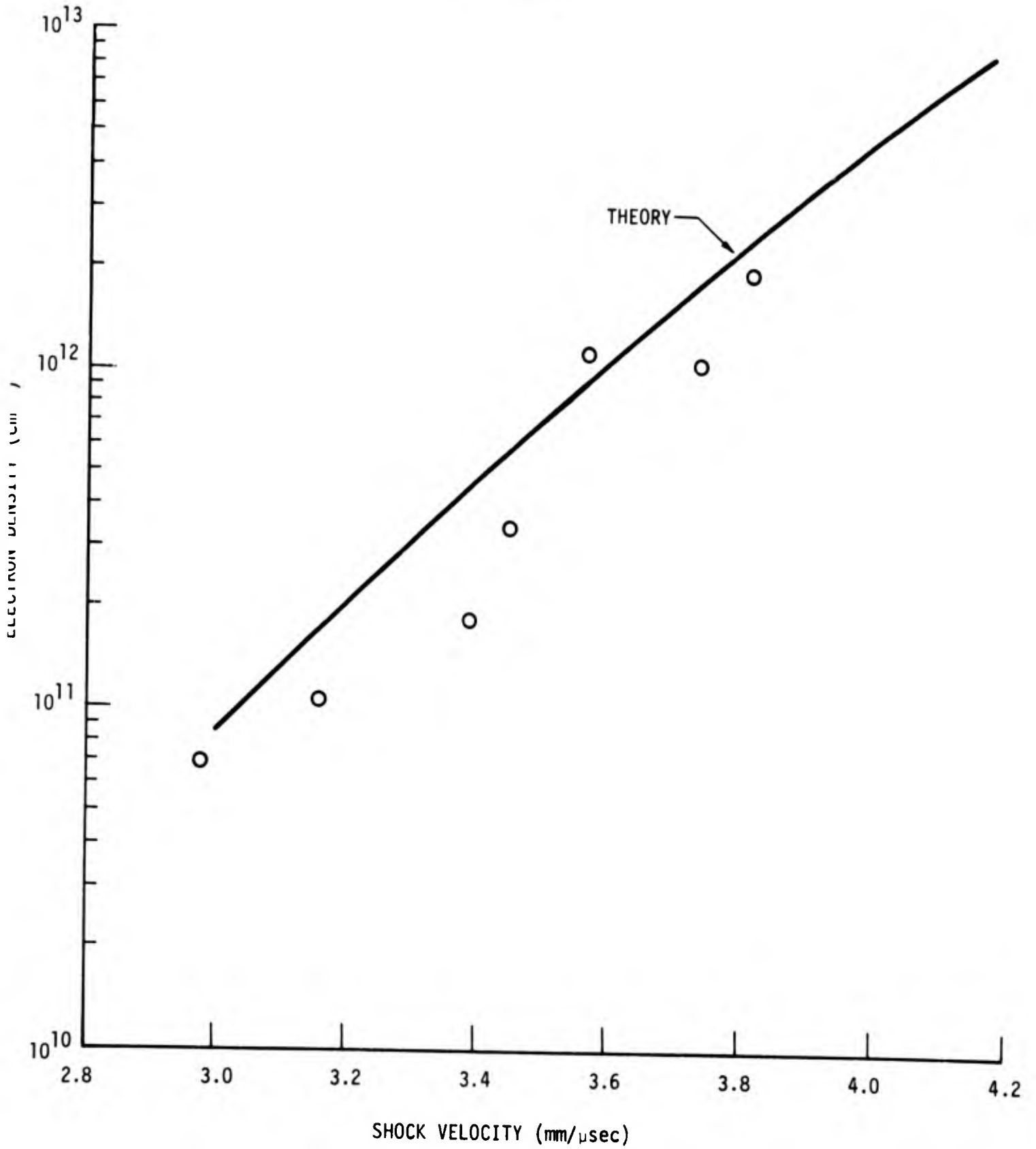


Fig. 8 ELECTRON DENSITY BASED ON ELECTRON CURRENT, P = 10 TORR

SHEATH LOCATION

PROBE BIAS -12 VOLTS  
INITIAL PRESSURE 5 TORR  
FLUSH PROBE

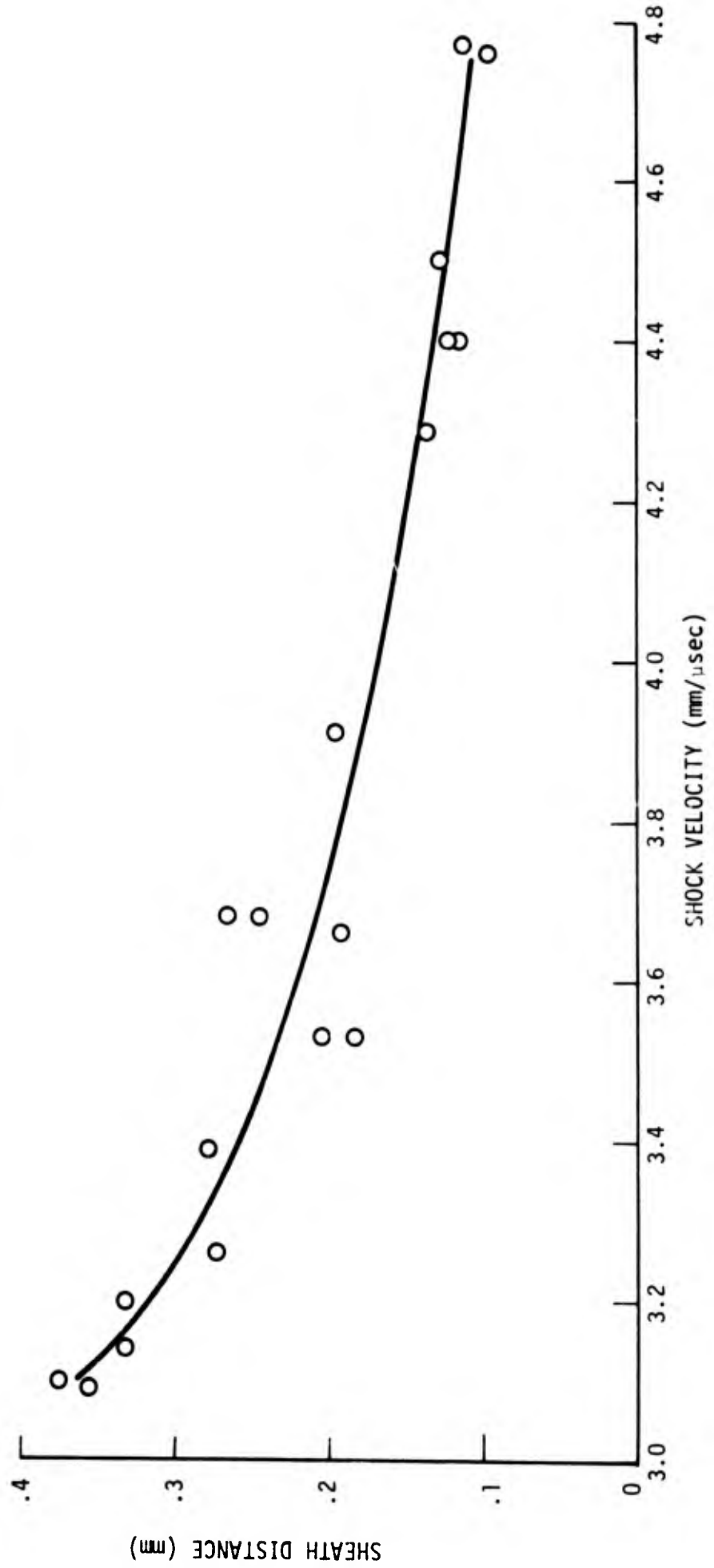


Fig. 9 SHEATH LOCATION, P = 5 TORR, V = -12 VOLTS

ELECTRON DENSITY  
BASED ON ION CURRENT

INITIAL PRESSURE 5.0 TORR  
PROBE BIAS -12.0 VOLTS  
FLUSH PROBE

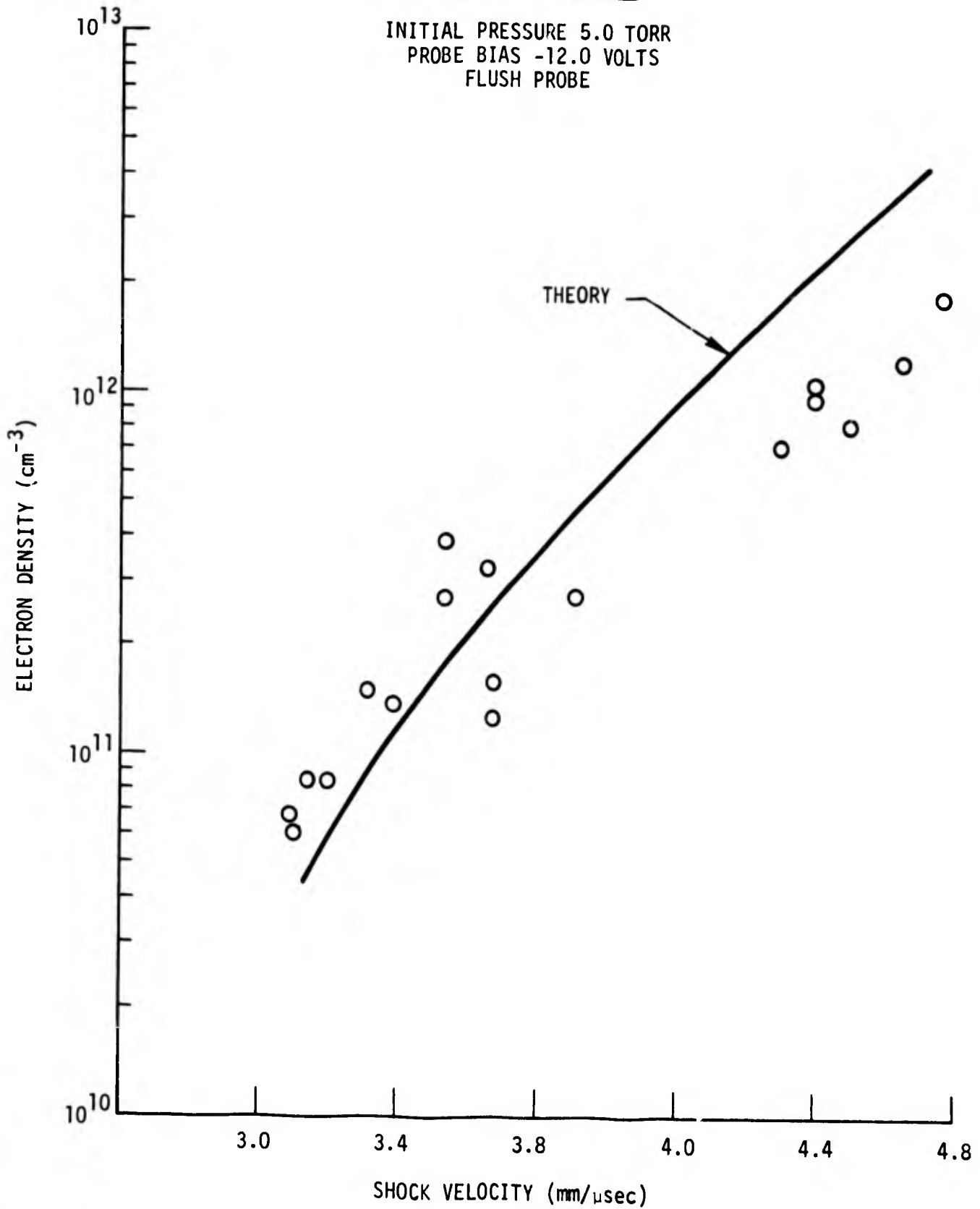


Fig. 10 ELECTRON DENSITY BASED ON ION CURRENT  
P = 5 TORR

in the circuit. A typical response of the probe is shown in Figure 11b. The velocity at the same axial location of the probe was also measured from the output of piezoelectric static pressure probes. The shock wave ahead of the stagnation point probe forms rapidly, and the flow relaxes to an equilibrium flow in a few microseconds.

#### 4.1 Stagnation Point Probe Theory

The probe theory used to define the flush mounted electrostatic probe was also used to define the stagnation point probe operation. The sheath edge was calculated with the same relation used to define the flush probe sheath edge. The full random flux was also assumed to be collected by the probe at the sheath edge. All properties were determined from conditions at the edge of the viscous layer.

#### 4.2 Stagnation Point Flow Field Theory

The flow surrounding the probe is the classical hypersonic stagnation point flow field. The most universally accepted solutions to the stagnation point problem are the solutions of Fay and Riddell<sup>19</sup>. The heat transfer through the boundary layer has been shown to be adequately predicted by a simple correlation formula. For an equilibrium boundary layer the Fay-Riddell formula presents a simple relation for Nusselt number. The Stanton number can then be calculated from the definition of Nusselt, Prandtl, and Reynolds numbers. With the aid of the modified Reynolds analogy between heat transfer and skin friction, a relation for the boundary layer momentum thickness can be obtained. The momentum thickness for a flow in which the Lewis number is unity is

$$\frac{\delta}{x} = 1.34 \left( \frac{\rho_s \mu_s}{\rho_w \mu_w} \right)^{.4} (R_e)^{-1/2} (P_r)^{-1/3}$$

where  $\delta$  = momentum thickness

$x$  = probe radius

$\rho$  = density

$\mu$  = viscosity

$R_e$  = Reynolds number

$P_r$  = Prandtl number

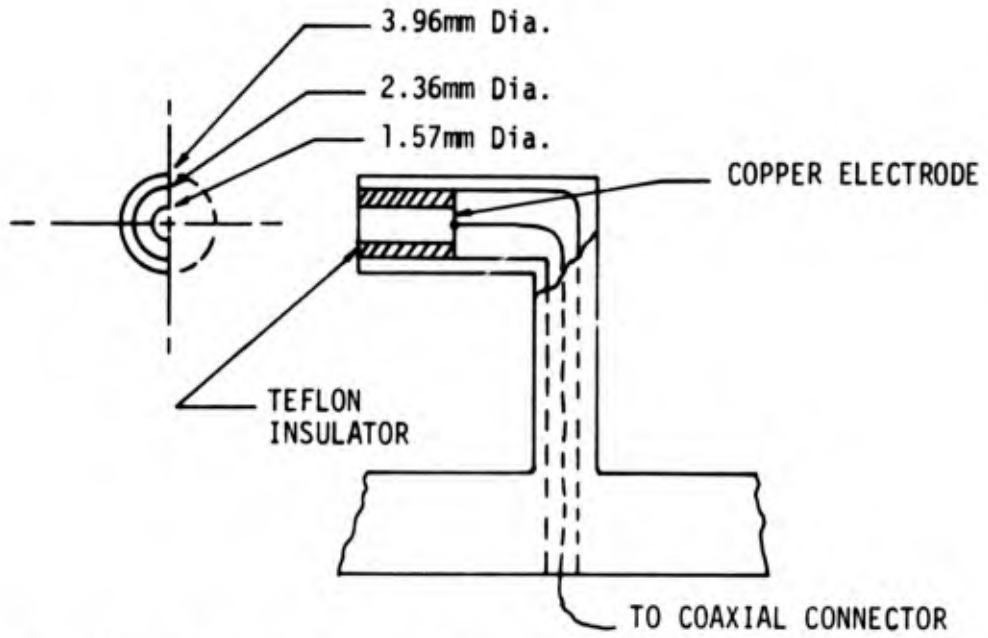


Fig. 11a STAGNATION POINT ELECTROSTATIC PROBE

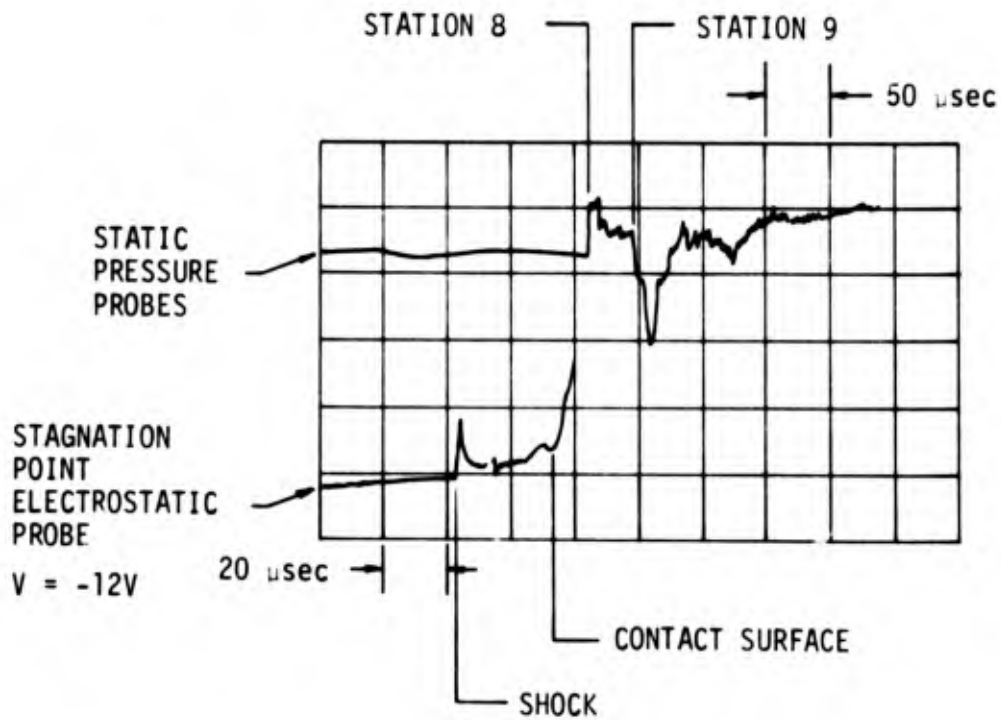


Fig. 11b STAGNATION POINT ELECTROSTATIC PROBE RESPONSE

and the subscript  $s$  refers to conditions at the edge of the boundary layer and the subscript  $w$  refers to conditions at the wall. With the assumption of a power law velocity profile a relation between the momentum thickness and boundary layer thickness can be established from their respective definitions<sup>20</sup>. An approximation to the velocity profile may be made from the similar solutions of Fay and Riddell. A power law variation of velocity profile with an exponent of  $1/4$  is an approximation which holds for 80% of the total profile. The enthalpy profile can now be calculated for the assumed velocity profile by using the Crocco integral method. The electron density at the sheath location can now be determined with the aid of real gas tables<sup>15,16</sup>.

#### 4.3 Stagnation Point Probe Measurements

Measurements of the probe current collected by a stagnation point probe located on the centerline of the rectangular test section were made. The shock tube initial pressure was maintained at 5 torr and the probe bias was set to -12 volts. The electron density and the sheath distance were calculated in the same manner as the flush mounted probes. The sheath location is shown in Figure 12 as a function of shock velocity for the experimental conditions. The electron density as deduced from the probe current measurements is shown in Figure 13 where the results are also compared with the theoretical predictions. The stagnation point probe electron density measurements appear to agree within a factor of three with the predicted values.

#### 5.0 CONCLUSIONS

Measurements of the electron density in a turbulent boundary layer have been performed with flush electrostatic probes for conditions typical of low altitude, high velocity reentry. The use of a simplified probe theory appears to agree with an engineering calculation of the electron density at the edge of the probe sheath. Owing to the many approximations used to define the boundary conditions, agreement within a factor of two is realized. Probes biased to collect ion current or electron current appear to give the same order of agreement.

SHEATH LOCATION

PROBE BIAS -12 VOLTS  
INITIAL PRESSURE 5 TORR  
STAGNATION POINT PROBE

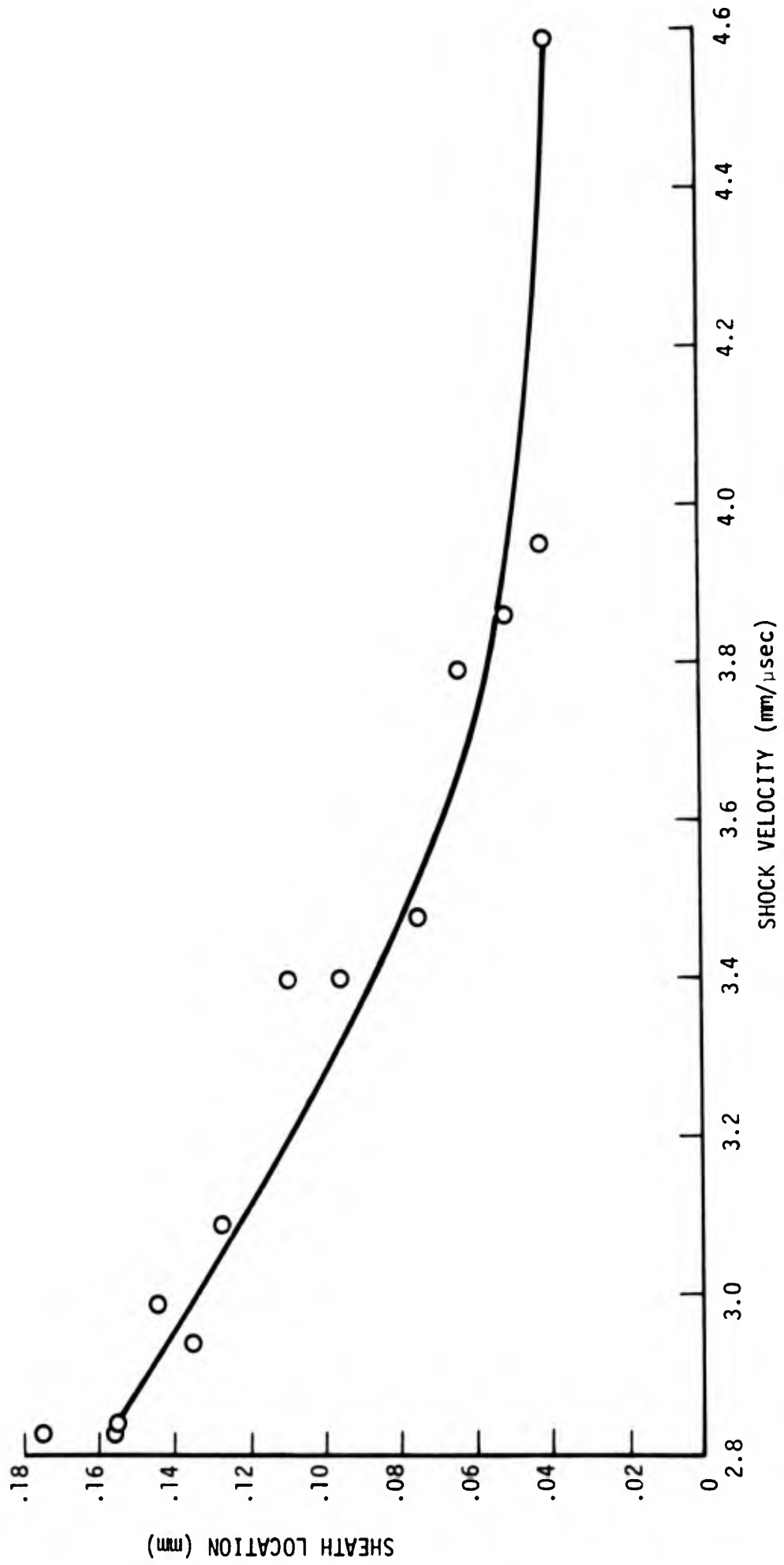


Fig. 12 SHEATH LOCATION, P = 5 TORR, V = -12 VOLTS

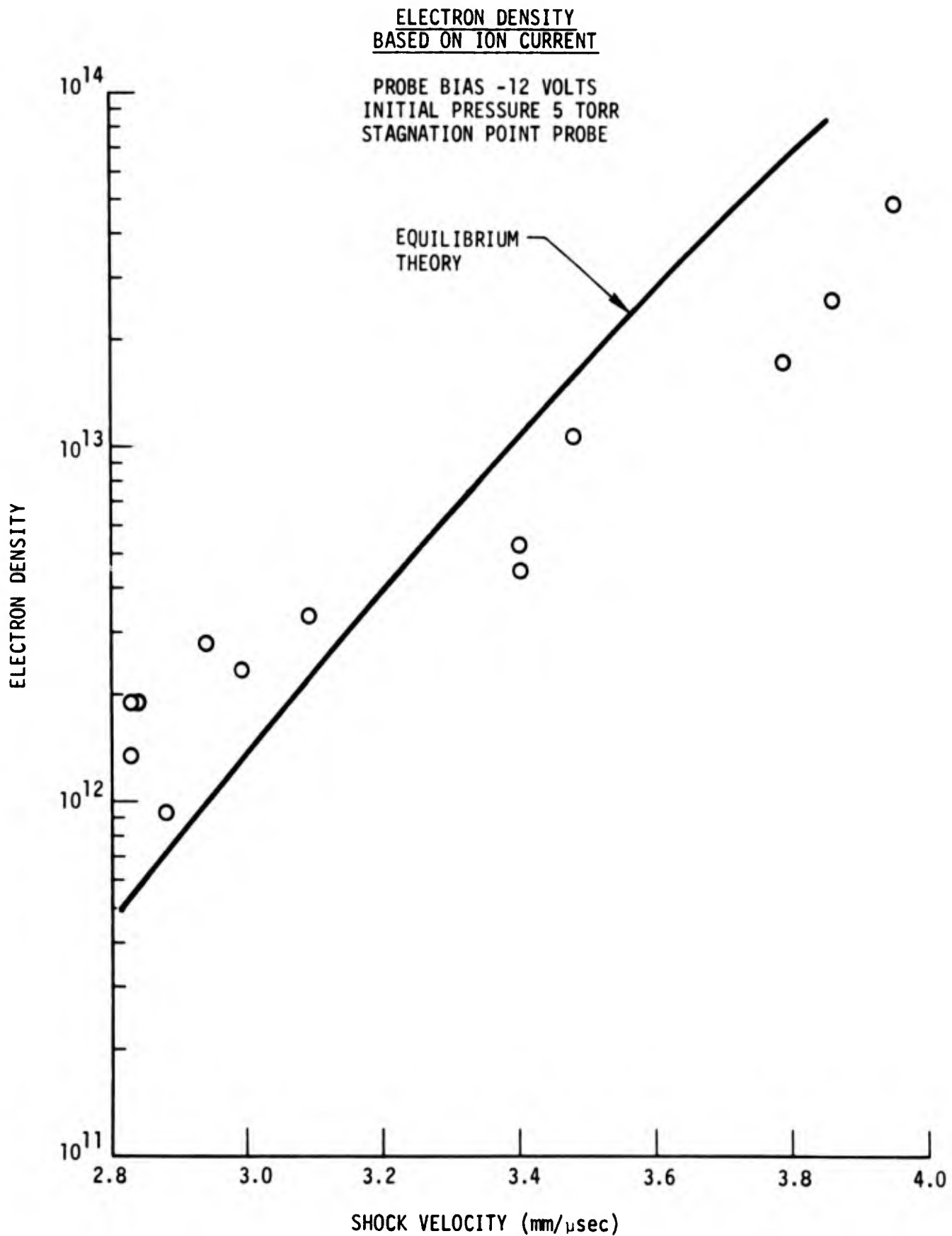


Fig. 13 ELECTRON DENSITY BASED ON ION CURRENT,  
P = 5 TORR, V = -12 VOLTS

The electron density in the stagnation point laminar boundary layer has also been measured. The measured electron density agrees within a factor of three with an engineering calculation of the stagnation point flow conditions.

The probe currents measured in these experiments are based upon mean currents collected by the probe over the available test time. The variation in the current collected by the flush electrostatic probes represent fluctuations in the ion density due to a turbulent boundary layer. Owing to the limitations of available test time in the shock tube flow, the observed ion current fluctuations correspond to frequencies above 100 kHz. The observed fluctuations appear to be relatively mild indicating a low spectral energy density. This observation is in agreement with detailed measurements of the spectral energy density of a turbulent plasma layer which indicate that the maximum energy density is contained in frequencies below 5 kHz<sup>21</sup>.

REFERENCES

1. Hayes, D. T., and Rotman, W., AIAA J. 2, 675 (1973).
2. Hayes, D. T., AIAA Paper No. 72-694, 1972.
3. Bredfelt, H. R., Scharfman, W. E., Guthart, A., and Morita, T., AIAA J. 5, 91 (1967).
4. Rudderow, W. H., Jour. of App. Phys. 43, 373 (1972).
5. Lederman, S., and Avidor, J., Israel J. of Tech. 9, 19 (1971).
6. Burke, A. F., AIAA Paper No. 68-166, 1968.
7. Chung, P. M., and Blankenship, V. D., AIAA J. 4, 442 (1966).
8. Hoppmann, R. F., Phys. Fluids 11, 1092 (1968).
9. Boyer, D. W., and Touryan, AIAA J. 10, 1667 (1972).
10. Russo, A. J., and Touryan, K. J., AIAA J. 10, 1675 (1972).
11. Cobine, J. D., Gaseous Conductors, p. 36, Dover, New York, 1958.
12. Mirels, H., AIAA J. 2, 84 (1964).
13. Menard, W. A. and Horton, T. E., NASA CR 106660, 1969.
14. Jacobs, H. R., "Engineering Approximations of the Effects of Blunting on Cones in Laminar and Turbulent Flow," Aerospace Report No. TR-0158 (S3816-41)-1, 1967.
15. "Thermodynamic Properties of High Temperature Air," Chance Vought Research Center Report RE-IR-14, 1961.
16. Logan, J. G. and Treanor, C. E., Tables of Thermodynamic Properties of Air from 300°K to 10,000°K at Intervals of 100°K, Cornell Aero. Lab. Report BE-1007-A-3, 1957.
17. Talbot, L., Phys. Fluids 3, 289 (1960).
18. Pollin, I., Phys. Fluids 7, 1433 (1964).
19. Fay, J. A. and Riddell, F. R., AIAA J. 25, 73 (1958).
20. Schlichting, H., Boundary Layer Theory, McGraw-Hill, 1960.
21. Chown, J. B., "Antenna Performance in the Presence of a Turbulent Plasma," Vol I NASA SP-252, 1970.